ARTICLE   OPEN

Check for updates

Advanced wastewater treatment and membrane fouling control by electro-encapsulated self-forming dynamic membrane bioreactor

Jessa Marie J. Millanar-Marfa[1,8], Mary Vermi Aizza Corpuz [ID][1,8], Laura Borea[2], Carlo Cabreros[1], Mark Daniel G. De Luna[1,3], Florencio Jr. Ballesteros[1,3], Giovanni Vigliotta[4], Tiziano Zarra[2,5], Shadi W. Hasan [ID][6], Gregory V. Korshin [ID][7], Antonio Buonerba [ID][4,5 ✉], Vincenzo Belgiorno[2] and Vincenzo Naddeo [ID][2,5 ✉]

An advanced concept of aerobic membrane bioreactors (MBRs) for highly efficient wastewater treatment has been disclosed by introduction of an electro and encapsulated self-forming dynamic biomembrane (e-ESFDM). The biological filtering membrane is intercalated between two woven polyester fabrics as supports that assist the formation and protect the biomembrane. The innovative architecture of the e-ESFDM in combination with electrocoagulation processes resulted in efficient and cost-effective wastewater treatment and control of the membrane fouling. The performance of the e-ESFDMBR was compared to a yet highly efficient ESFDMBR, where the electric field was not present. The ESFDM-based reactors both showed comparable results in the removal of organic matter, in terms of COD and DOC. On the other hand, e-ESFDMBR exceeded the performance of the ESFDMBR in the reduction of nitrogen- and phosphorous-containing pollutants, responsible for eutrophication processes in the environment, and recalcitrant molecules, such as humic-like substances. In addition, an extremely low fouling rate was observed for the e-ESFDM bioreactor. Insights on the biological processes involved in the developed MBR were provided by investigations on the microbiological diversity found in reactor mixed liquor, ESFDM layer and treated wastewater.

INTRODUCTION

Aerobic and anaerobic membrane bioreactors (MBRs) are efficient systems for wastewater treatment[1–3]. Their performance largely exceeds that of traditional wastewater treatment systems.

In MBRs, wastewater treatment occurs passively in conventional ultra- and micro-filtration modules (with pore sizes in the ranges 1–100 nm and 0.1–10 μm, respectively). Efficient wastewater treatment in MBRs occurs via membrane filtration on the MBR modules. While efficient, these systems are prone to clogging and decrease in permeate flux due to membrane fouling. In addition, MBRs are also limited by high operational and capital cost. In response to these challenges cheaper materials with higher pore sizes such as woven and non-woven fabric[4–6] were used as alternative materials to membrane modules.

The biofilm contains microorganisms that, fed by the wastewater nutrients, produce the living filtering material and afford the wastewater treatment. Aerobic SFDMBRs show excellent results for the removal of organic matter from wastewater, with reduction efficiencies of chemical oxygen demand (COD) and dissolved organic carbon reductions (DOC) of 89–99% ca[7–11]. SFDMBRs are also efficient for the removal of ammonia nitrogen compounds (ammoniacal nitrogen, NH_3-N, also referred as ammonium-nitrogen, NH_4^+-N) with removal efficiencies in the range 76–99%. However, they have relatively low overall efficiencies for the other forms of nitrogenous compounds and

the total nitrogen (TN) removal efficiencies are in the range of 21–80%[7–11]. SFDMBR systems are also not yet capable of efficiently removing phosphate-phosphorus (PO_4^{3-}-P)[12] and the range of the total phosphorus (TP) removal rates in SFDMBR operations is in the range of 6–27%[13–15].

Recent studies have shown that the introduction of an electric field and electrochemically controlled processes in conventional membrane bioreactors (e-MBRs) improved the removal efficiency of PO_4^{3-}-P up to 96%[16]. Electrochemical oxidation of the anode in the examined reactor resulted in the release of aluminium or iron ions and resulted to the precipitation of insoluble phosphates. In turn, these precipitates triggered the consequent removal via coprecipitation of some recalcitrant organic pollutants and emerging contaminants such as pharmaceutical compounds[17] and even pathogen microorganisms, such as bacteria and viruses[18,19]. Similar studies by Zhang et al.[20] and Ibeid et al.[21] reported for this class of bioreactors respectively 30% and 67% of reduction in membrane fouling, as a result of the decrease of soluble microbial products (SMP) acting as fouling precursors. The integration of electrochemical processes with MBRs has been shown to reduce membrane fouling rate due to several electrochemical and electrokinetic phenomena such as electro-coagulation, electroosmosis, and electrophoresis[22]. In addition, the application of electric field in MBRs has been recently shown to reduce membrane fouling rate through the reduction of quorum

[1]Environmental Engineering Program, National Graduate School of Engineering, University of the Philippines, 1101 Diliman, Quezon City, Philippines. [2]Sanitary Environmental Engineering Division (SEED), Department of Civil Engineering, University of Salerno, Via Giovanni Paolo II, 84084 Fisciano, Italy. [3]Department of Chemical Engineering, University of the Philippines, 1101 Diliman, Quezon City, Philippines. [4]Department of Chemistry and Biology "Adolfo Zambelli", University of Salerno, 84084via Giovanni Paolo II, Fisciano, Italy. [5]SPONGE s.r.l, Corporate Spin-off of University of Salerno, via Giovanni Paolo II, 84084 Fisciano (SA), Italy. [6]Center for Membranes and Advanced Water Technology (CMAT), Department of Chemical Engineering, Khalifa University of Science and Technology, Abu Dhabi PO Box 127788, United Arab Emirates. [7]Department of Civil and Environmental Engineering, University of Washington, Box 352700, Seattle, WA 98105-2700, USA. [8]These authors contributed equally: Jessa Marie J. Millanar-Marfa, Mary Vermi Aizza Corpuz. ✉email: abuonerba@unisa.it; vnaddeo@unisa.it
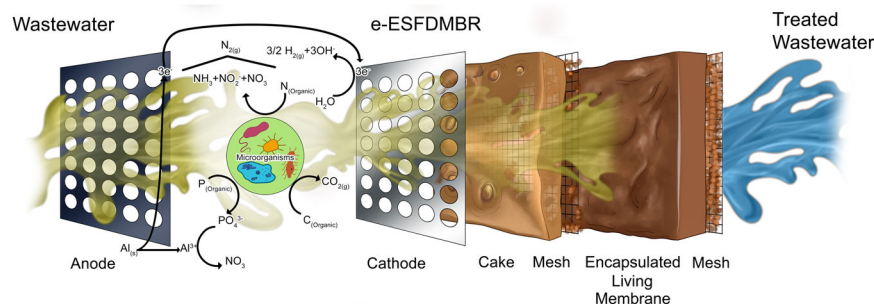
Fig. 1 e-ESFDMBR. Synoptical view of the chemical, physical and biological processes occurring in the e-ESFDMBR.

sensing (QS) signal molecules; this effect has been correlated with the reduction of concentration of fouling precursors[23,24]. Finally, the quality of the flocs in e-SFDMBRs in part improve the stability and prevent the removal of the SFDM from the membrane.

The current study describes a system for wastewater treatment where the SFDM that formed during the operation of a bioreactor is encapsulated between two woven polyester meshes, in the presence of an applied electric field generated between an aluminium electrode, as an anode, and a steel cathode electrode (Fig. 1). This study aims to utilize the new system called encapsulated self-forming dynamic membrane bioreactor (e-ESFDMBR) to treat wastewater and compare its performance to an identical ESFDMBR where there is no applied electric field in terms of removal of wastewater pollutants such as nutrients (TN and TP), COD and DOC and fouling control. In addition, it also aims to investigate the difference in DM morphology, presence of fouling precursors and structure and diversity of microbial community and their corresponding impacts on the performance of the two systems (e-ESFDMBR and ESFDMBR).

RESULTS AND DISCUSSION

The experimental setup adopted in this study is depicted in Fig. 2 and described in the experimental section. The effective formation of the ESFDM can be quantified by monitoring permeate flux, transmembrane pressure (TMP), and effluent turbidity. A decrease of the permeate flux that requires an increase of the transmembrane pressure (TMP) in order to keep the flow constant, accompanied by a reduction of effluent turbidity are indicative for the formation of the ESFDM. The ESFDMBR, compared to a conventional MBR[25], allows a higher filtration flux (15 LMH for the conventional MBR and 30 LMH for ESFDMBR). The large pore size of the Dacron mesh compared to conventional membranes permitted longer operation time with minimal filtration resistance.

Permeate turbidity values below 5 NTU are unambiguously indicative of the effective formation of SFDMs[26]. The time-course monitoring of the permeate turbidity of e-ESFDMBR in comparison with that for ESFDMBR is shown in Fig. 3a. The turbidity of the effluent from the e-ESFDMBR rapidly dropped below the unit value within the first day of operations of the reactor (green plot in Fig. 3a). Values below 5 NTU were found for the permeate of ESFDMBR only after 7 days of its operations (red plot in Fig. 3a). The quality of the permeate was very high and constant for the entire time of the e-ESFDMBR operations, with turbidity values close to those for clean water, which demonstrates the efficiency and stability of the encapsulated dynamic biomembrane of the e-ESFDMBR. The average turbidity values for ESFDMBR and the e-ESFDMBR were 3.87 ± 1.34 NTU and 0.21 ± 0.09 NTU; the latter value corresponds to a $99.29 \pm 0.31\%$ turbidity reduction efficiency (see Supplementary Table 1).

The difference in turbidity reduction efficiency can be explained by the shift in particle size distribution once an electric field in the e-ESFDMBR was applied. In the presence of an electric field,

electrolytic oxidation of aluminium anode occurred forming aluminium ions that led to destabilization and precipitation of phosphates (vide infra) and organic pollutants in water. This resulted to the formation of larger flocs formed through electrocoagulation. This can be observed in the increase in particle size distribution (see Supplementary Fig. 1). The larger flocs in the e-ESFDMBR resulted in less particles passing through the ESFDM layer and carried to the effluent, and in lower turbidity values. In addition, the higher turbidity values after ~28 days of operation in the ESFDMBR effluent may be attributed to the detachment of some particles in the ESFDM layer because of compression due to the high TMP values (see also discussion in the subsection on Transmembrane Pressure). The higher TMP in the reactor without applied electric field may have potentially caused breakage in some portions of the ESFDM layer and resulted in some particles carried to the effluent, increasing the turbidity. However, it is to be noted that the turbidity values in the ESFDMBR remained to be still below 5 NTU throughout the operation due to the reformation of the living membrane during wastewater treatment.

The rapid formation of the SFDM in the e-ESFDMBR can be explained by taking into account the different size distributions of the particulate present in the reactors. The application of the electric field in the e-ESFDMBR rapidly causes the electrocoagulation of phosphates in the form of aluminium/phosphate solid phases (see Fig. 1 and further the discussion concerning the fate of phosphates nutrients). It also causes partial coagulation of some organic pollutants present in the wastewater, with the resulting formation of flocs with larger sizes. The flocs thus generated can start accumulating in the filtering module, with the resultant formation of the SFDM. The analysis of the particle size distributions (PSD) of the cake and ESFDM layers confirmed this assumption. The particles present in the cake layer of the e-ESFDMBR showed a size distribution curve shifted to a larger size, compared to that in the ESFDMBR, as shown in Supplementary Fig. 1a, b. On the other hand, as expected considering the pore size of the Dacron® support, the PSDs of the ESFDM layer for both reactors resulted similar with the maximum of the curve distribution at c.a. 30 μm (Supplementary Fig. 1c, d) that is close to the pore size of the mesh support used for the growth of the ESFDM. Changes in the PSD in the presence of an electric field and lower filtration resistance at higher PSD were demonstrated in the previous studies[22,27]. Further contributions in the mitigation of the membrane clogging are associated with electrophoresis and electroosmosis processes, where the negatively charged foulants were driven towards the positively charged anode, preventing their adhesion to the ESFDM surface. At the same time, the positively charged wastewater pollutant was driven towards the cathode and the ESFDM layer[22,28].

The TMP values for the e-EFSDMBR were lower than those for the ESFDMBR which, in turn, were significantly lower than those observed for conventional MBRs[11]. The plot of TMP over time (Fig. 3b) showed a continuous increase in the TMP of the ESFDMBR
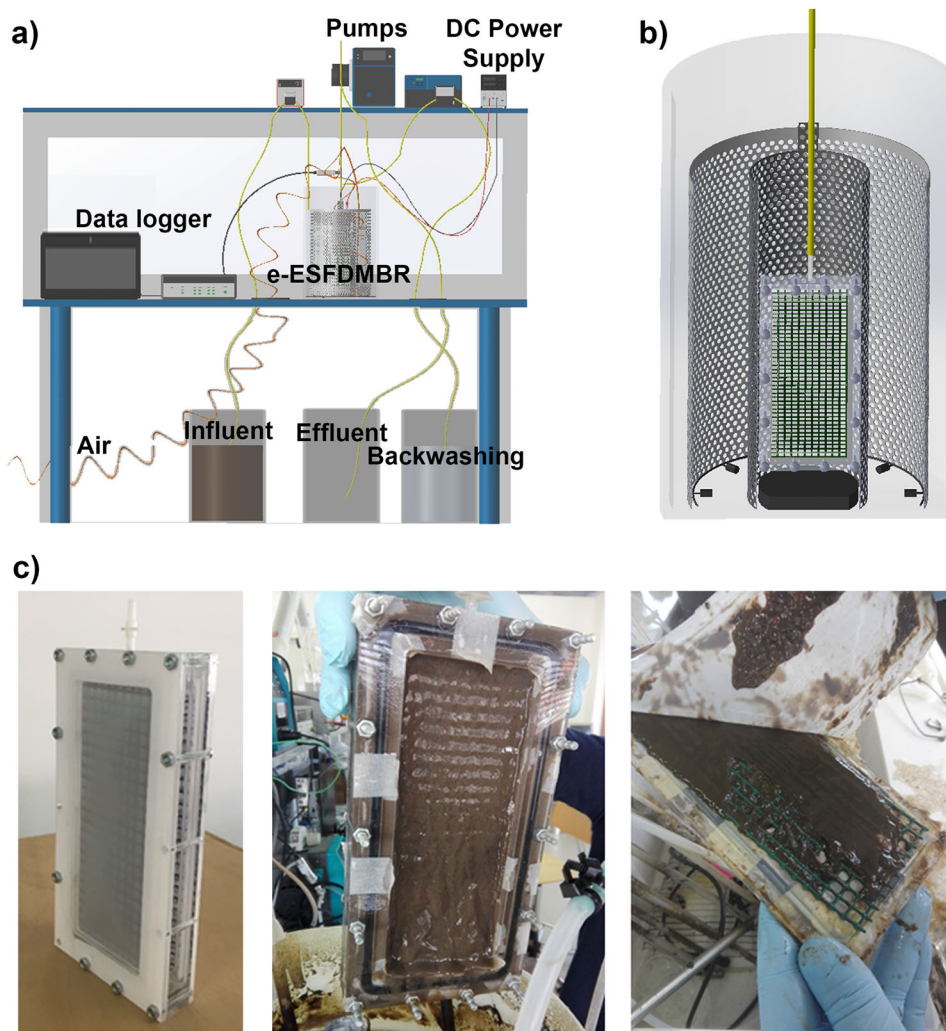
Fig. 2 e-ESFDMBR. Experimental setup of e-ESFDMBR (**a**). Cross-section of the bioreactor (**b**). Photographs of the e-ESFDM module before and after operation in the bioreactor and finally showing the formed ESFDM (**c,** Philippines).

during the first 18 days of operation. The TMP of the ESFDMBR even reached a maximum of 2.30 kPa during the operations. The TMP in the e-ESFDMBR increased in the first hours of operation and was relatively constant afterwards, reaching only a maximum of 1.5 kPa c.a., which was lower than that of the ESFDMBR. The TMP values for the e-EFSDMBR were constant in a range close to 1 kPa, indicating an optimal operation of the filtering module (Fig. 3b). Low TMP values which were always accompanied by a high quality of the permeate are attractive practically because they are indicative of the lower energy consumption needed for the suction of the permeate and, thus, for low costs of operation of the MBR. The stability of the encapsulated living biomembrane is further supported by the nearly constant TMP observed during the entire operation time of the e-ESFDMBR (Fig. 3b). In contrast to the stability observed in the e-ESFDMBR, the TMP profile of ESFDMBR showed continuous increase during the first 39 days. The TMP values in the ESFDMBR started to decrease after this period, implying possible detachment of some portions of the ESFDM layer because of compression due to the initially high values of TMP. After ~50 days, the TMP in the ESFDMBR started to rise again to values close to those observed in the e-ESFDMBR due to further deposition of substances on the ESFDM layer, being a dynamic membrane, as operation of the reactor continued. The average fouling rates of ESFDMBR and e-ESFDMBR were 0.105 and 0.032 kPA/d, respectively (see Experimental section for the

determination of this values). This demonstrates again that electric field application improved membrane filterability by inducing electrocoagulation, electroosmosis and electrophoresis[21,29] and decreasing the concentration of fouling precursors (Fig. 3), as discussed in more detail below.

Fouling precursors whose behaviour in EFSDMBR and e-EFSDMBR is compared in Fig. 3 (see additionally Supplementary Table 2) are products of microbial communication known as QS. This process enables microorganisms to excrete QS substances called autoinducers to produce a synchronized response such as biofilm formation. In a previous study by Borea et al.[23], electric field application improved fouling mitigation through a process called quorum quenching (QQ) which reduced the concentration of C8-HSL, a QS substance frequently related to SMP and EPS concentration[30]. Significant reduction in average SMP_p (65.4%), SMP_c (78.1%), EPS_p (76.1%), EPS_c (72.3%) and TEP (25.4%) concentrations obtained in the e-ESFDMBR can then be associated with three processes, (1) biodegradation in the bioreactor and the ESFDM layer, (2) electrocoagulation (destabilization, adsorption, flocculation) and (3) possible occurrence of QQ which prevents fouling precursor generation.

Sludge relative hydrophobicity (RH) of ESFDMBR(63.4%) was also higher than that of e-ESFDMBR(32.50%). Hydrophobic sludge has a higher tendency to adhere on the surface of the mesh support and cause fouling[31]. A study by Lei et al.[32] reported a
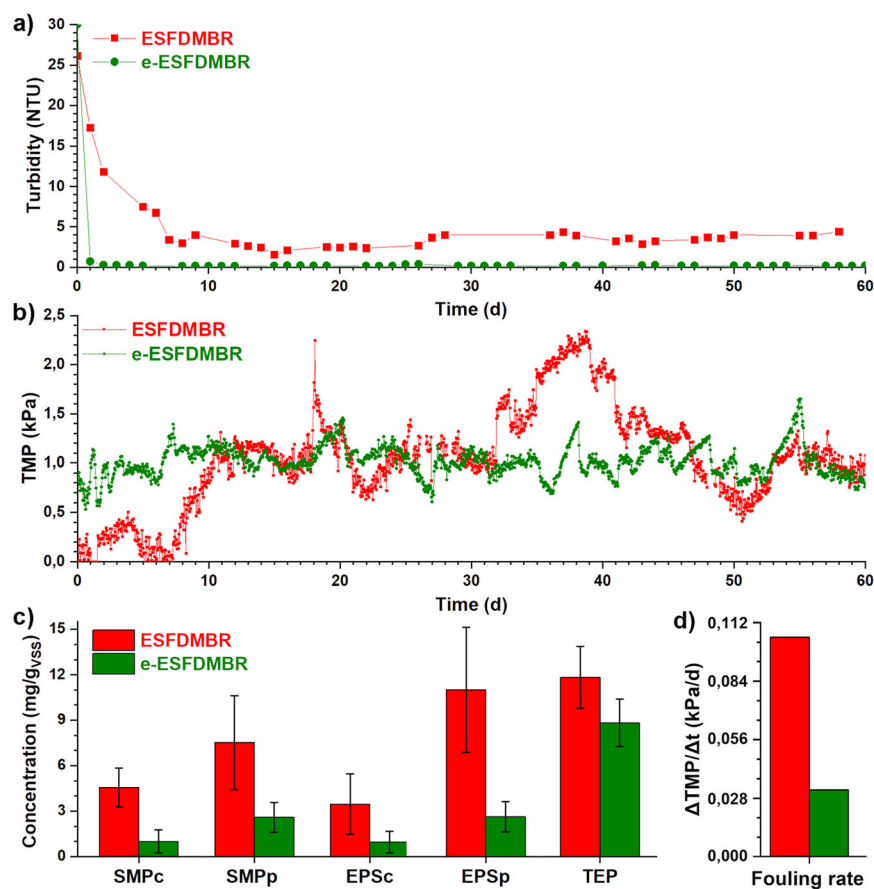
Fig. 3 SFDM formation and fouling mitigation indicators. Time profiles of effluent turbidity (panel **a**) and TMP (panel **b**) from the ESFDMBR and e-ESFDMBR as indicators of the rapid formation of the encapsulated SFDM in e-ESFDMBR. Fouling precursor tri-weekly (three times a week) average concentrations and fouling rates (panel **c**, **d**, see additionally Supplementary Table 2). Error bars in panel **c** show the standard deviations.

significant correlation between SMP concentration and sludge properties such as RH, thus, a reduction in RH could be accounted for the decrease in SMP concentration brought upon by electrochemical processes.

The morphology of SFDM and cake layers formed in the ESFDMBR and e-ESFDMBR was explored by scanning electron microscopy, SEM (Fig. 4). The layers were gently cut from the filtering module, crosslinked with glutaraldehyde in order to preserve the native morphology, dried by sequential treatment with an aqueous solution of ethanol with increasing concentration of the alcohol and final drying by treatment with supercritical carbon dioxide. Both ESFDM (Fig. 4a, b) and cake (Fig. 4c, d) layers of the ESFDMBR showed a compact morphology with a prominent accumulation of remnants of amoebas and diatoms. The ESFDM in the e-ESFDMBR (Fig. 4e, f) also showed a compact morphology with a reduced accumulation of amoebas and diatoms. The partial removal of the ESFDM from the Dacron® support (Fig. 4i, j) provided information on the mechanism of occlusion and formation of the SFDM in e-ESFDMBR. The microorganisms generated fibrillar structures, which, in combination with the retained particulates, generated a network capable of occlusion of the Dacron® pores. A fibrillar morphology, with large pores and with an almost absent accumulation of amoebas and diatoms, was found for the cake layer on the e-ESFDMBR filtering module (Fig. 4g, h). The compact morphology of the ESFDMs operated both with and without applied electric field explains the good performance of these bioreactors, while the enhanced porosity of the cake layer in the e-ESFDMBR accounts

for the improved control on the TMP and thus on the fouling observed for this reactor.

The ESFDM-based bioreactors, besides the removal of colloidal particles and particulates, as shown in the section on the reduction of effluent turbidity, were also found to be highly effective in the removal of chemical contaminants from the wastewater. Time-course monitoring of the most important and indicative parameters for the efficiency of MBRs for wastewater treatment are reported in Fig. 5 and Supplementary Table 4.

The removal of PO_4^{3-}-P is a strong indicator of the efficacy of MBRs with electrocoagulation processes. In fact, a limited removal of orthophosphate was observed for the ESFDMBR(average removal of $14.2 \pm 9.3\%$) while PO_4^{3-}-P was completely removed in the e-ESFDMBR (>99.9%, Fig. 5a, i and Table S4). Phosphate removal in the e-ESFDMBR can be attributed to both biotic and abiotic processes. Polyphosphate-accumulating organisms (PAOs) present in activated sludge contribute to the removal of PO_4^{3-}-P from wastewater (vide infra). In the case of the e-ESFDMBR, PO_4^{3-}-P removal could also be due to the electro-generation of $Al(OH)_3$[33] and subsequent precipitation of the solid phase of aluminium phosphate $AlPO_4$[25,34,35]. We believe that the precipitation of PO_4^{3-} appears to be the potentially dominant removal pathway of PO_4^{3-} from wastewater in e-ESFDMBR. In the presence of electric field application, the electrochemical oxidation and resultant release of aluminium to Al^{3+} takes at the anode (Fig. 1). The electrochemically generated Al^{3+} cations readily react with PO_4^{3-} solutes to form precipitates. Aluminium release from the anode also results in the formation of aluminium hydroxide flocs which further contribute to the removal of wastewater
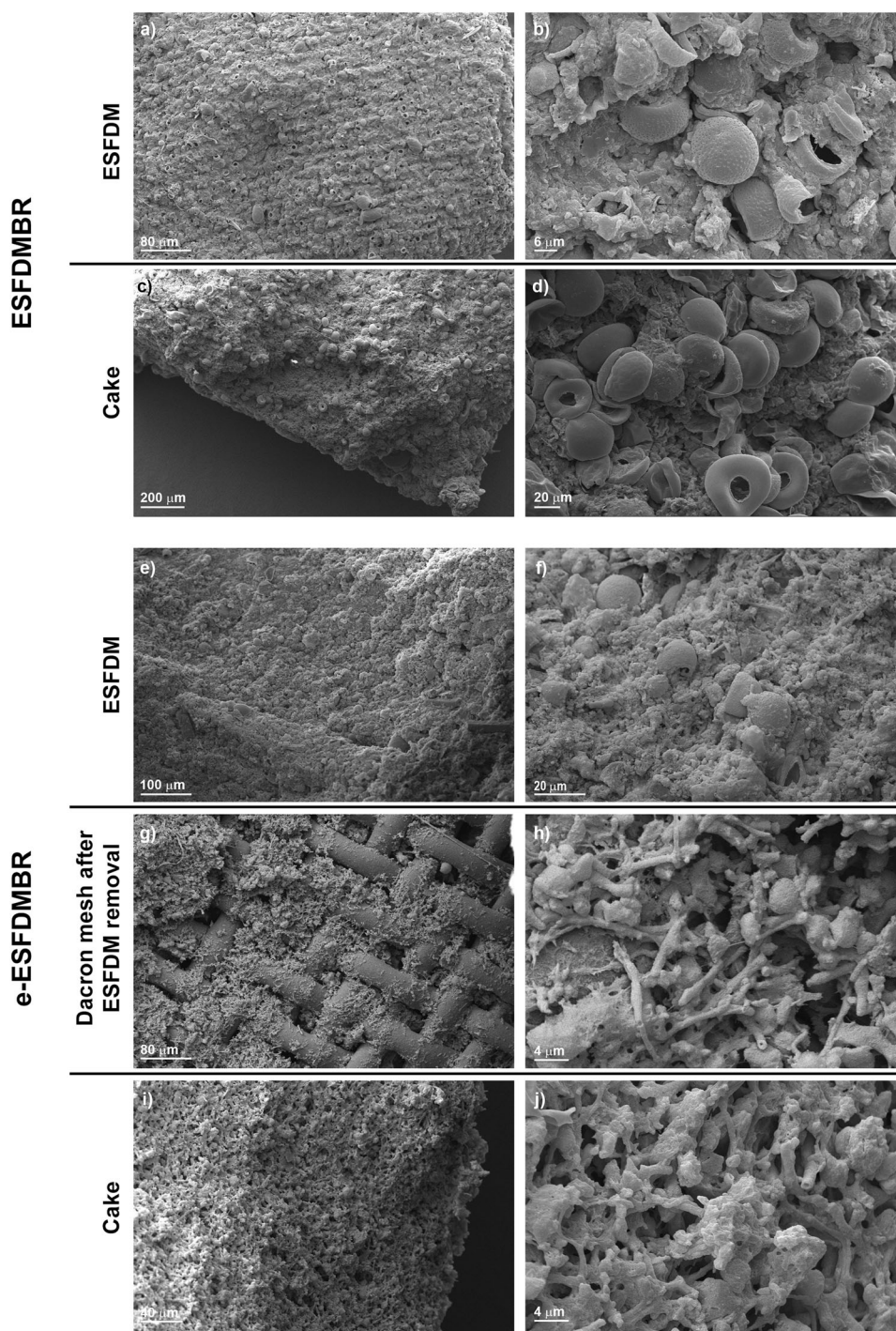
Fig. 4 Morphology of SFDM and cake layers by SEM. ESFDMBR: ESFDM (**a**, **b**) and cake (**c**, **d**). ESFDMBR: ESFDM (**e**, **f**), Dacron® mesh after partial removal of the ESFDM (**g**, **h**) and cake (**i**, **j**).

contaminants. Measurements of Al concentration confirm the extent of this process. During the e-ESFDMBR operations, the aluminium concentration increased from the initial value of 20.64 mg/L to 1248 mg/L found at the end of the runtime. This confirms the accumulation of this aluminium in the bioreactor.

The monitoring of chemical oxygen demand (COD, Fig. 5a) and dissolved organic carbon (DOC, Fig. 5b) demonstrated that the performance of the ESFDM-based bioreactors in the removal of organic matter exceeded that of the conventional activated sludge processes and aerobic membrane bioreactors. High efficiencies in COD reduction ($94.8 \pm 3.4\%$ for ESFDMBR,

$99.4 \pm 0.3\%$ for e-ESFDMBR) and DOC removal ($93.08 \pm 1.27\%$ for ESFDMBR, $97.47 \pm 0.6\%$ for e-ESFDMBR) were found for the bioreactors. The e-ESFDMBR experiments showed the rapid formation of the SFDM, which exhibited a high degree of detention of organic matter in the bioreactor and also enabled its degradation to carbon dioxide, as shown in Figs. 1 and 5a. The excellent performance observed for the e-ESFDMBR can be ascribed to the electrocoagulation processes occurring in this reactor. The adsorption of organic matter to the particulate matter, as well as to the electrochemically generated aluminium hydroxide and aluminium phosphate solids, improves the
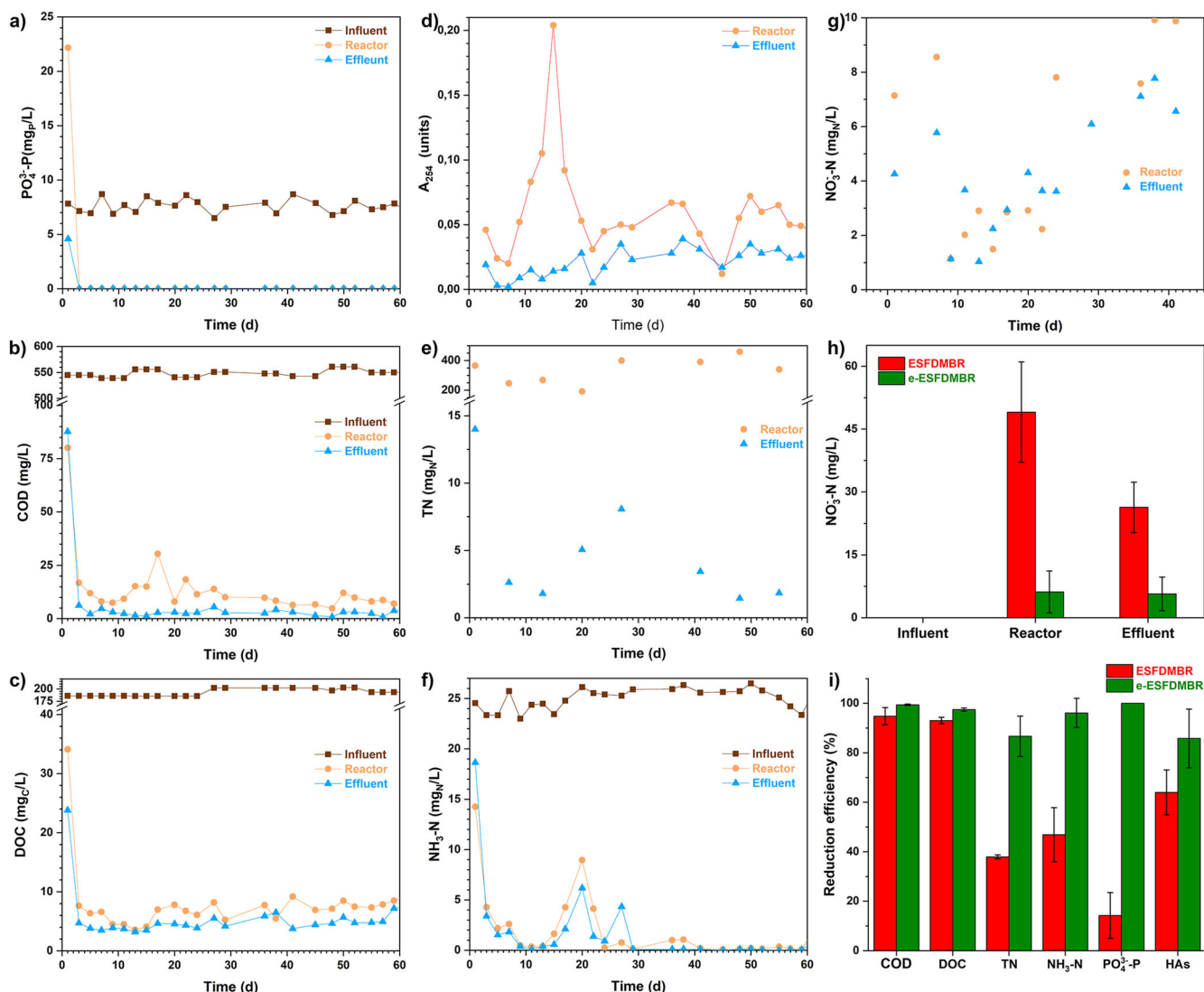
Fig. 5   Removal of wastewater contaminants by e-ESFDMBR. Time-course monitoring of: **a** phosphate phosphorous (PO_4^{3-}-P), **b** chemical oxygen demand (COD), **c** dissolved organic carbon (DOC), **d** UV absorbance at wavelength of 254 nm (A_{254}), **e** total nitrogen (TN), **f** ammonia nitrogen (NH_3-N), **g** nitrate nitrogen (NO_3^--N). NO_3^--N concentrations from influent to effluent in ESFDMBR and e-ESFDMBR (**h**). Overall reduction efficiencies of wastewater pollutants by ESFDMBR and e-ESFDMBR (**i**).

detention of these compounds in the reactor and the following degradation by microorganisms.

The improved detention of organic matter in the e-ESFDMBR is supported by measurements on the absorbance at the wavelength of 254 nm (A_{254}, Fig. 5c) for the bioreactor and the effluent. The A_{254} parameter is an indicator for the concentration of wastewater organic matter present in, in particular of humic acid-like substances (HAs)[36,37].

It is essential for wastewater treatment process to remove these substances as they may increase the fouling propensity in membrane systems[38,39] or may react with active chlorine to produce potentially carcinogenic substances[40].

For the e-ESFDMBR, the peak A_{254} values were found during the first 20 days of bioreactor operation. This indicates an accumulation of organic matter and recalcitrant substances during this period. However, the A_{254} values for the effluent were very low during the same and the following period, indicating that the dynamic membrane is effective in the detention of organic matter, including HAs in the bioreactor, largely preventing its release in the effluent. A 21.8% improvement in the removal of HAs, represented by the absorbance at 254 nm, was observed when

the electric field was turned on. This change may be associated with the enhanced removal of HAs due to charge neutralization and rapid sweep coagulation[41,42].

The fate of nitrogen-containing compounds in the ESFDMBR and e-ESFDMBR was more complex. NH_3-N average removal of $46.9 \pm 11\%$ for the ESFDMBR was relatively low when compared with the results in prior studies where the reported removal efficiencies were in the range 76–99%[7,9,10]. In contrast, an excellent NH_3-N removal efficiency of $96.0 \pm 4\%$ was obtained for the e-ESFDMBR. Nitrate concentrations in the mixed liquor and effluent of the e-ESFDMBR were similar, suggesting for this contaminant an "apparent" little or none at all removal. However, the NO_3^--N concentrations were very low, below 10 mg/L (Fig. 5g). The overall removal of nitrogen-containing compounds, expressed as total nitrogen (TN), was very high of $86.7 \pm 8.2\%$ (Fig. 5e and Table S4). The TN concentrations in the reactor were very high and constant (200–400 mg/L, see Fig. 5e) during its operation. The release of TN in the effluent was initially high (15 mg_N/L c.a.) which corresponded to the NH_3-N concentration (Fig. 5e, f). Ammonia present in the influent is the first intermediate of the biological cascade reactions for the decomposition of nitrogen-containing
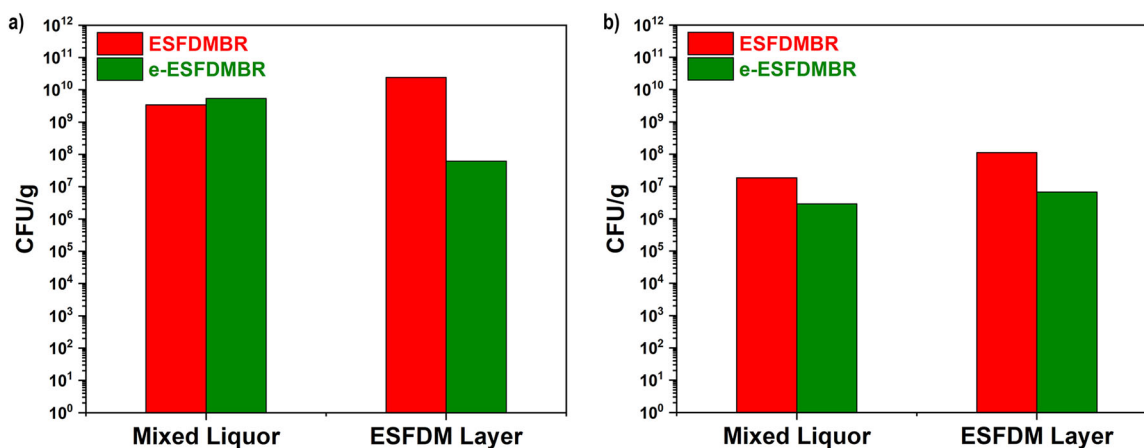
Fig. 6 Density of culturable microorganisms. Comparison of total cell count (**a**) and endosporeforming bacteria count (**b**) in the ESFDMBR and e-ESFDMBR. Colony forming units (CFU) are referred to dry weight (grams) of layer and mixed liquor.

pollutants of wastewater and it can pass through the filtering module when the ESFDM had not yet been formed. The growth in the bioreactor of microorganisms able to convert ammonia to nitrate, together with the formation of the ESFDM, reduces the release of ammonia in the effluent (Fig. 5f). The similar concentrations of nitrate in bioreactor and effluent indicate that this anion easily passes through the ESFDM. On the other hand, the low concentrations of nitrate, in the order of a few milligrams per litre (Fig. 5g), indicates that nitrate was not accumulating in the reactor. This indicates that the nitrate is likely to be an intermediate and it was sufficiently rapidly converted into gaseous nitrogen and released into the atmosphere. Therefore, nitrogen is mostly present in the bioreactor in the form of biomass or organic matter adherent to the flocs of the sludge.

Nitrogen removal consists of nitrification and denitrification processes. The nitrification process requires aerobic conditions for the conversion of ammonium nitrogen to nitrate (NO_3^-) while denitrification commonly requires anoxic conditions for the conversion of NO_3^- to N_2 gas.

In this study, both ESFDMBR and e-ESFDMBR were operated under aerobic conditions. Nonetheless, continuous monitoring of redox potential, ORP and DO concentration in the bioreactors showed that once the electric field was turned on, the e-ESFDMBR became anoxic. This is consistent with the findings of previous studies[17,25]. The average ORP values and DO concentration decreased from 268 mV and 6.5 ppm, respectively, when the electric field was turned off to 2.7 mV and <1 ppm, respectively when the electric field was turned on. The anoxic condition in the e-ESFDMBR significantly favoured the denitrification process, as illustrated by the relatively lower NO_3-N concentration in the reactor and effluent of the e-ESFDMBR compared to the ESFDMBR (Fig. 5).

The higher removals of both NH_3-N and NO_3^--N in the e-ESFDMBR are likely due to a combination of better retention and the occurrence of alternating aerobic and anoxic conditions in the bioreactor during the intermittent application of the electric field. This also resulted in a significant improvement in TN removal. In addition, a study by Wang et al.[43] reported the growth of nitrifiers and denitrifiers on the cathode side, their presence supporting higher removal of nitrogen in the e-ESFDMBR. The present study also detected the presence of these microorganisms in the e-ESFDMBR, as will be discussed in more detail in the subsequent section.

The density of total cultivable microorganisms in the mixed liquor of the e-ESFDMBR was higher by <1-log$_{10}$ than that in the mixed liquor of the ESFDMBR (Fig. 6a and Supplementary Table 5). This slight increase in the mixed liquor is consistent with the

results of the study by Zeyoudi et al.[44], where the application of low current density (0.5 to 2.0 mA/cm^2) resulted in an increase in the bacterial count and the bacteria's oxygen uptake rate (OUR). However, in the previous study, the identities of the specific bacteria, whose count were increased by the electric field application, were not determined.

The density of total cultivable microorganisms in the ESFDM layer of the e-ESFDMBR was lower by 2-log$_{10}$ compared to that obtained in the ESFDM layer of the ESFDMBR (Fig. 6a). In the e-ESFDMBR, the microbial count was also significantly lower in the ESFDM layer than in the mixed liquor. The intensity of the electric field in the zone where the ESFDM layer was located was lower than that in the mixed liquor. The external cake layer and the bilayer structure of the membrane module provided a protection for the ESFDM layer from the applied electric field. This implies that the very low intensity of the electric field in the encapsulated SFDM layer of the reactor was not enough (compared to that in the mixed liquor) to enhance the total bacterial growth.

The counts of endospore-forming bacteria, in contrast to the trend observed for the total bacterial density, in both the mixed liquor and ESFDM layer were reduced in the presence of an electric field (Fig. 6b).

The data on microbial density should be complemented with the data on the distribution of microorganisms in terms of class/species in the ESFDMBR and e-ESFDMBR to better understand the effect of the electric field on the microorganisms.

In both the ESFDMBR and e-ESFDMBR, it was observed that proteobacteria was the most dominant phylum. This agreed with the results of analysis of microbial communities in aerobic submerged MBRs, in which proteobacteria was dominant in the biofilm formed on the membrane surface and in the activated sludge[45–47]. The abundance of proteobacteria in biofilms suggested their importance in biofilm formation and their contribution to biofouling in conventional MBRs[45]. The results in the present study also revealed that the presence of electric field led to the decrease in the fraction of proteobacteria in the e-ESFDMBR (69.84%) compared to that obtained in the ESFDMBR (85.25%). In a previous study that compared the microbial communities of an aerobic ceramic MBR (with and without the presence of an electric field), it was observed that the phylum proteobacteria was slightly decreased in the reactor with electric field[48], the application of an electric field to the reactor resulted in a shift in the structure of the community of microorganisms at different taxa levels, as reported for endospores forming Firmicutes (Fig. 7). The fraction of phylum of proteobacteria was higher in the e-ESFDMBR, both in mixed liquor and ESFDM layer. A significant increase in the fraction of γ-proteobacteria class was observed in the mixed liquor of the
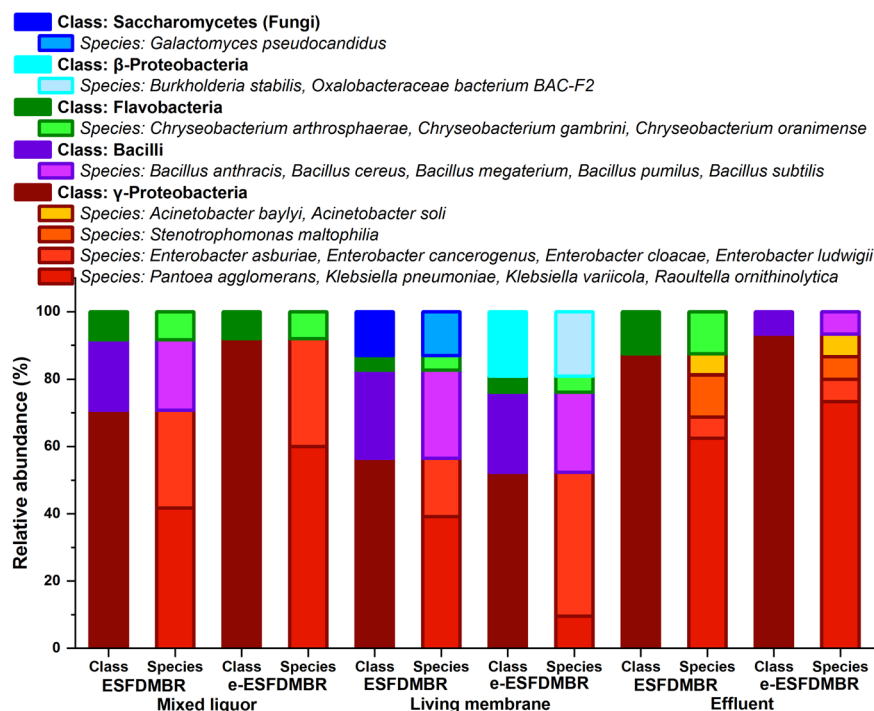
Fig. 7 Microbiological investigation. Class and species distribution of cultivable microorganisms in ESFDMBR and e-ESFDMBR in the corresponding mixed liquor, living membrane biofilm and effluent (see additionally Supplementary Tables 6, 7).

e-ESFDMBR compared to the fraction in the mixed liquor of the ESFDMBR (Fig. 7). In particular, the relative abundance of the group containing the *Pantoea agglomerans*, *Klebsiella pneumoniae*, *Klebsiella variicola*, and *Raoultella ornithinolytica* accounted for almost all the increase of this bacterial class (Fig. 7). On the other hand, the fraction of γ-proteobacteria was comparable in the ESFDM layer of both reactors (52.4% and 56.5%). Contrarily, to the mixed liquor, a large reduction in the relative abundance of the group of *Pantoea agglomerans*, *Klebsiella pneumoniae*, *Klebsiella variicola*, and *Raoultella ornithinolytica* species was observed in the presence of an electric field (ESFDM layer: 39.13%, e-ESFDM layer: 9.52%). This significant reduction was compensated by a high increase in the fraction of the species belonging to the genus *Enterobacter* (ESFDM layer: 17.39%, e-ESFDM layer: 42.86%) so that the relative abundance of γ-proteobacteria remained unchanged in both the reactors. The growth of *β-proteobacteria* was also promoted in the ESFDM layer of the e-ESFDMBR. On the other hand, it was not identified anywhere in the ESFDMBR, most likely due to low abundance. This class of bacteria has been recently identified as dominant in membrane biofilms[49]. In summary, the conditions established in the e-ESFDM reactor, significantly influenced the phylum of proteobacteria, favouring the growth of the group of *Pantoea*, *Klebsiella*, and *Raoultella* spp. in the mixed liquor, and that of *β*-proteobacteria and *Enterobacter* genus in the ESFDM layer.

The structure of the community of microorganisms in the dynamic membrane was different from that in the mixed liquor. This is consistent with results reported in previous studies on conventional submerged MBRs, in which differences in the structure of microbial communities in the fouling layer and in the activated sludge were observed[50,51]. In the e-ESFDMBR, a marked difference in the distribution phylum, class and species was observed between the ESFDM layer and the bulk liquid. As discussed, the lower relative abundance of the species *Pantoea agglomerans*, *Klebsiella pneumoniae*, *Klebsiella variicola*, and *Raoultella ornithinolytica* and a higher fraction of the genus *Enterobacter* were observed in the ESFDM layer than in the mixed

liquor. This showed the higher tendency of the *Enterobacter spp.* to adhere to and colonize the ESFDM layer. Endospore-forming bacteria, such as those belonging to the genus *Bacillus*, have been reported to have hydrophobic spores, which allows them to adhere to surfaces[52]. The hydrophobicity of the surface of spores formed by bacteria of the genus *Bacillus* suggests that these microorganisms are important in the formation of biofilm and may contribute to membrane fouling. Bacteria of the genus *Bacillus* were present in the mixed liquor and ESFDM layer of the ESFDMBR. However, in the e-ESFDMBR, the *Bacillus* species were only detected in the ESFDM layer. This observation implied the effect of the application of electric field in the reduction of population of the mentioned species. The ESFDM layer was enclosed in a chamber and was shielded by another external cake layer, and its structure may have provided protection to the bacteria of genus *Bacillus* from the applied electric field. On the other hand, the bacteria in the mixed liquor were directly exposed to the electric field, which potentially inhibited their growth. The count of these bacteria of genus *Bacillus* were reduced upon the application of electric field. This is seen in the count of endospore-forming bacteria, which decreased in the e-ESFDMBR in comparison to that observed in the ESFDMBR (Fig. 6b). This reduction of bacteria with hydrophobic spores in the reactor could have potentially contributed to the decrease of the fouling rate. The population of endospore-forming bacteria extracted from the total cultivable microbiota after heat treatment was represented by *Bacillus* species. The growth of *Bacillus spp.* was more promoted in the ESFDM layer than in the mixed liquor of the e-ESFDMBR (see Fig. 7). The lower density in the e-ESFDMBR could explain the absence of this genus in the microbiota isolated from e-ESFDM mixed liquor without heat pre-treatment selection (Fig. 7). However, the promotion of growth of some *Bacillus spp.* in the ESFDM layer compared to that in the mixed liquor may have also helped in the mitigation of membrane fouling. *Bacillus cereus* and *Bacillus subtilis* have been identified as bacteria that produce N-Acyl homoserine lactone (AHL)-lactonase, an enzyme that degrades AHLs[53–55]. AHLs are signal molecules that bacteria use
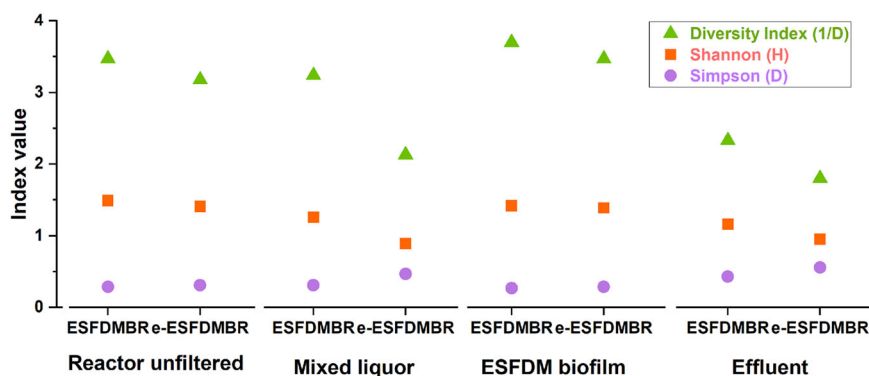
Fig. 8 Microbial diversity. Diversity indices of the cultivable microbial community in ESFDMBR and e-ESFDMBR (see additionally Supplementary Table 8).

to coordinate their behaviour, such as biofilm formation. Higher AHL concentrations have also been shown to correlate with higher concentrations of membrane fouling precursors[23,56,57]. Thus, the presence of some *Bacillus spp*. in the ESFDM layer may have contributed to the reduction of AHLs in the e-ESFDMBR, to the reduction of EPS and SMP concentrations, and subsequently to the reduction of membrane fouling rate.

The differences in prevailing biological conditions, hydrodynamic conditions, and intensity of electric field between the mixed liquor and ESFDMBR have resulted in a difference in the structures of microbial communities in the mixed liquor and dynamic membrane, and subsequently, have influenced the membrane fouling mitigation.

Figure 8 and Supplementary Table 8 show that the overall diversity indices (H and 1/D) for the ESFDMBRare higher than for the e-ESFDMBR. This implies that the application of electric field decreased the diversity of cultivable microorganisms in all zones in the reactor.

It is also noted that the diversities of the cultivable microbial community in the ESFDM layers of both the ESFDMBR and e-ESFDMBR are higher than those of the communities in their corresponding mixed liquors. This suggests that the ESFDM layer generally supports the growth of more types of bacterial species than the corresponding mixed liquor does. This also implies that the ESFDM layer protection from external stressors, thus promoting the prevalence of more types of species compared to the mixed liquor.

The removal of nitrogen and phosphorus from the wastewater in the e-ESFDMBR is realized mainly by biological and electrochemical processes. The sequencing described in the preceding sections revealed the presence of nitrifying and denitrifying bacteria in the system. Strains of *Klebsiella pneumoniae* and *Klebsiella variicola* have been previously identified as both heterotrophic nitrifiers and aerobic denitrifiers[58,59]. The abundance of these bacteria in the mixed liquor may have contributed to the removal of nitrogen through nitrification and aerobic denitrification. Although the group of *Klebsiella pneumoniae* and *Klebsiella variicola* species have a lower relative abundance in the ESFDM layer, their presence is still important since they can still provide additional nitrogen removal as the wastewater flows through the matrix. It has been previously reported that the metabolism of nitrifying bacteria present in a biofilm formed on a surface was less affected by the application of electric field than that of the bacteria in bulk sludge[60]. Thus, the decrease of nitrification rate of the nitrifying bacteria in the ESFDM layer due to the application of electric field could be less than what is observed in the mixed liquor.

A strain of *Enterobacter cloacae* has been previously reported to be a polyphosphate-accumulating organism (PAO)[61]. Strains of *Enterobacter cloacae* were also observed to be capable of removal of nitrogen from wastewater samples by heterotrophic nitrification and aerobic denitrification[61,62]. The presence of *Enterobacter cloacae* in the mixed liquor implies that aside from nitrification, and denitrification under anoxic conditions, another possible pathway of nitrogen removal is through denitrification in the presence of O_2.

Perspective

In this study, a new system called e-ESFDMBR was developed by augmenting the ESFDMBR reactor with electrochemical processes. Intermittent application of a 0.5 mA/cm² current density induced a combination of electrocoagulation, electroosmosis and electrophoresis inside the e-ESFDMBR. This noticeably improved the efficiency of the e-ESFDMBR compared to a conventional ESFDMBR in terms of TN, NH_3-N, PO_4^{3-}-P and humic substances removal by 48.7%, 49.2%, 85.8% and 21.8%, respectively. The average fouling rate was reduced from 0.105 kPa/d in the ESFDMBR to 0.032 kPa/d in the e-ESFDMBR. The improvement in fouling mitigation was validated by the reduction in fouling precursors concentration and sludge relative hydrophobicity. Nonetheless, the study measured the combined influence of electrocoagulation, electroosmosis and electrophoresis on contaminant removal and membrane filterability. To further understand the effect of electric field application on contaminant removal and membrane filterability and to further optimize the process, it is recommended that future studies measure the individual effects of each mechanism.

Microbiological analyses revealed that the application of electric field led to increased microbial counts in the mixed liquor and decreased microbial count in the ESFDM layer. The application of electric fields also led to a decrease in the overall diversity of microorganisms in the reactor. However, the decrease in microbial diversity did not lead to a reduced performance of the e-ESFDMBR. The growth of more types of species was observed to be promoted in the ESFDM layer compared to those in the mixed liquor. The microbiological analyses also showed that the microbiological community present in the different zones of the e-ESFDMBR affected pollutant removal and membrane fouling mitigation. Next-generation sequencing (NGS) is recommended in further studies to provide a complete analysis of the microbiological community and its influence on the performance of the e-ESFDMBR.

This study shows that the e-ESFDMBR can be a promising alternative to conventional MBR systems.

The application of electric field to drive the electrochemical processes in the e-ESFDMBR requires additional energy input. However, it is worth noting that the current density magnitude used was low at 0.5 mA/cm² and was applied intermittently, which may contribute to the reduction of energy consumption due to

the application of electric field. The present study did not measure the specific energy consumption of the e-ESFDMBR. In previous studies on electrochemical MBRs, the energy used to drive electrochemical reactions added 2.38% to 10% to the total energy consumption, in which more than 50% was attributed to aeration[20,63]. The energy E utilized to drive the electrochemical processes may be estimated using the following equation[64]:

$$E = \frac{VI}{1000 * Q}$$

where E = energy consumption in kWh/m^3 of treated water, V = generated voltage in volts, I = current in Amperes, and Q = treated water flowrate in m^3/hr. Using the measured average voltage 0 f 8.6 V, current density of 0.5 mA/cm^2 applied intermittently with the cycle of 5 min ON/20 min OFF, and treated wastewater flowrate of 0.642 L/h, a specific energy consumption (to drive electrochemical process) of 4.42 kWh/m^3 was calculated. This calculated value is higher than that obtained by Mendes Predolin et al.[64]. However, in the previous study, the estimated specific energy consumption of 0.26 kWh/m^3 (for the power applied to electrodes) was calculated for a pilot-scale plant with a larger volume of treated wastewater. In another study, Ibeid et al.[21] consumed ~0.6–2.0 kWh/m^3 of energy when an operation mode of 5 min ON/15 min OFF and 5 min ON/20 min OFF. This energy consumption is comparable to what was obtained in this study. Furthermore, energy consumption for intermittent electric field application may still be reduced with optimization studies. In their study, Bayramoglu et al.[65] noted that the cost of operating aluminium anode electrocoagulation increases when the mixed liquor pH increases.

It is recommended in future studies to determine the actual specific energy consumption in e-ESFDMBRs, with the breakdown in energy usage associated with aeration, application of electric field, operation of pumps, and others. In addition, the lifespan of the electrodes and the concentration of aluminium in the effluent must be investigated in future studies.

METHODS

Materials

Chemical reagents and consumables were purchased from commercial sources (Merch, Sigma-Aldrich, Carlo Erba, TCI Chemicals, WWR Chemicals). Synthetic municipal wastewater was prepared according to the previously reported procedure[11,66] with the following composition: glucose ($C_6H_{12}O_6$, 200.0 mg/L), sucrose ($C_{12}H_{22}O_{11}$, 200.0 mg/L), proteins (68.3 mg/L), ammonium sulphate (($NH_4)_2SO_4$, 66.7 mg/L), ammonium chloride (NH_4Cl, 10.9 mg/L), potassium dihydrogen phosphate (KH_2PO_4, 4.44 mg/L), dipotassium hydrogen phosphate (K_2HPO_4, 9.0 mg/L), magnesium sulphate heptahydrate ($MgSO_4 \cdot 7H_2O$, 21.0 mg/L), manganese(II) sulphate heptahydrate ($MnSO_4 \cdot H_2O$, 2.7 mg/L), sodium bicarbonate ($NaHCO_3$, 30.00 mg/L), calcium chloride hexahydrate ($CaCl_2 \cdot 6H_2O$, 19.74 mg/L), iron(III) chloride hexahydrate ($FeCl_3 \cdot 6H_2O$, 0.14 mg/L)[11,16,23,66–70]. Dacron® mesh was provided by Saati s.p.a. (Appiano Gentile, Italy). Deionized water was produced from tap water with an Arium® Mini deionizer from Sartorius (Germany). The activated sludge, as inoculum for the bioreactors, was obtained from the recirculation line of the secondary clarifier stage of a municipal wastewater treatment plant in Salerno, Italy. DNA extraction and amplification of isolated and purified colonies were conducted using a REDExtract-N-Amp Plant PCR Kit (Merck Life Science Srl, Milan-Italy). Plate Count Agar (PCA: 5 g peptone, 2.5 g yeast extract, 1 g D-glucose, 15 g agar, 1 L deionized water) and Yeast Extract Peptone Dextrose (YEPD: 20 g D-glucose, 20 g Peptone, 10 g yeast extract, 20 agar, 1 L deionized water) were purchased from Sigma-Aldrich.

Experimental setups and operating conditions

ESFDM and e-ESFDM bioreactors with largely identical geometries were investigated in parallel under aerobic conditions (Fig. 2a, b). The synthetic municipal wastewater with composition shown in Supplementary Table 3 was continuously fed to the bioreactors. The cylindrical bioreactors were made of poly(methyl methacrylate) (PMMA) with an effective volume of

19 L. The filtration module consisted of a rectangular PMMA frame bearing the Dacron® mesh with a pore size of 30 µm and an effective filtration area of 0.021 m^2 was placed at the center of each cylindrical PMMA bioreactor (Fig. 2c). The design of the filtering module allows the formation of the living SFDM between two Dacron® meshes (pore size of 30 µm). The encapsulated SFDM is thus protected from the stresses induced by aeration and backwashing. Aerobic conditions were maintained by air diffusers placed at the bottom of the bioreactor. Metering Qdos 30 pumps from Watson-Marlow were used for permeate suction. 323S peristaltic pumps from Watson-Marlow were used for feeding the MBRs of influent and backwashing of the filtering modules. Effluent fluxes were 30 LMH and HRT used was 25 h[16,18,66]. A 10 min filtration cycle (9 min of filtration and 1 min of backwashing) was applied. The TMP was continuously monitored using a PX409-015VI digital pressure transducer from Omega (USA) connected to a 34972 A LXI data acquisition and switch unit from Agilent (CA, USA) and a computer for data recording. The e-ESFDM bioreactor was additionally equipped with two concentrical cylindrical perforated electrodes. These electrodes were a stainless-steel cathode, located internally next to the membrane module, and an aluminium anode, placed externally towards the wall of the bioreactor. The electrodes were connected to a CPX400S 420 W DC power supply from Aim-TTI Instruments (United Kingdom). A current density of 0.5 mA/cm^2, corresponding to a voltage of 8.6 V, was intermittently supplied for 5 min every 20 min, in agreement with a previous study[16].

Analytical methods

Samples from the influent, bioreactor and effluent were collected daily. Chemo-physical parameters such as pH, temperature, DO and ORP were constantly monitored using a HI769828 multiparametric probe from Hanna Instruments (RI, USA). Turbidity was measured with a 2100 N turbidimeter from HACH. Mixed liquor suspended solids (MLSS) and mixed liquor volatile suspended solids (MLVSS) were determined according to standard methods (APAT and CNR- IRSA 2003)[71]. The values of COD, DOC, TN, NH_3-N, NO_3^--N and PO_4^{3-}-P were measured using standard methods[71]. DOC concentrations were determined with a HyperTOC analyzer from Thermo Fisher Scientific equipped with an UV reactor and two infrared detectors. The samples were filtered (filter pore sizes of 0.45 µm) before measurements. DOC values were determined as the difference between total dissolved carbon (TDC) and total dissolved inorganic carbon (TDIC). TDC values were determined by treatment under UV radiation of 1000 µL of the sample with 1500 µL of a sodium persulphate solution (0.5 M) in combination with 1000 µL of a nitric acid solution (18%). TDIC values were determined by treatment of 1000 µL of the sample with 1000 µL of a nitric acid solution (18%). Instrumental calibration was performed analyzing standard solutions of potassium acid phthalate, sodium bicarbonate and sodium carbonate. NO_3^--N and PO_4^{3-}-P concentrations were determined by an ICS-90 ion chromatograph from Dionex, equipped with an IonPac AS9-HC column from Thermo Fisher Scientific and an AS40 automated sampler. Ion chromatographic measurements were performed with an injection volume of 10 µL, at a flow rate of 1.0 mL/min with an aqueous solution of sodium carbonate 9.0 mM as eluent. Concentrations of humic substances were estimated as absorbance values at a wavelength of 254 nm (A_{254}) determined with a Lambda 12 UV–Vis spectrophotometer from Perkin-Elmer, (Germany). Samples of mixed liquor from the bioreactor were filtered (pore size of 1.2 µm) before the measurement of the A_{254} absorbance values. The TMP was continuously monitored using a pressure transducer (PX409-0-15VI, Omega) connected to the membrane module. A data logger (34972 A LXI data acquisition/switch unit, Agilent) was used to record the TMP data obtained. The fouling rate was expressed as the variation of TMP over time

$$\text{Fouling rate} = \Delta TMP / \Delta t \qquad (1)$$

where: ΔTMP = change in membrane pressure (kPA) and Δt = time (d)).

Fouling precursors, namely TEP, EPS and SMP were monitored three times a week. TEP was analysed following the method established by previous studies[16,72]. SMP and EPS were extracted using heating methods[73,74] and their respective concentrations were quantified using photometric methods[75,76] using bovine serum albumin (Sigma, USA) and D-glucose (Sigma, USA) as standards. Fouling precursor concentrations were then normalized by using the concentration of MLVSS. Aluminium concentration in bioreactor mixed liquor were determined by inductively coupled plasma optical emission spectroscopy (ICP-OES) with an iCAP600 spectrometer from Thermo-Fischer. The sample (50 mL) was mineralized by sequential treatment with concentrated sulphuric acid

(20 mL) at 250 °C, with hydrogen peroxide (35%, 10 mL) at room temperature, and with hydrochloric acid (37%, 20 mL), and finally diluted with deionized water. The instrumental calibration was performed by analysing seven solutions prepared by progressive dilution of an aqueous aluminium (1000 g/L) standard solution. A FE-SEM LEO 1525 from Carl Zeiss SMT (Oberkochen, Germany) was used for scanning electron microscopy. The samples for SEM analysis were prepared as follow. In order to preserve the morphology of the ESFDM, specimens were gently cut from the module, fixed with an aqueous solution of glutaraldehyde (2.5 wt%), washed with phosphate buffer solution (PBS, 0.1 M, pH 7.2), progressively dehydrated by treatment in sequence with 25, 50, 75 and 98% ethanol aqueous solutions for 10 min each time. The specimens were, finally, anhydrified and volatile compounds eliminated by treatment with supercritical carbon dioxide, deposed on aluminium stubs and analysed. SEM analysis was carried out both for the sludge layer that formed the ESFDM between the two Dacron® support meshes (internal layer) and for the sludge layer that made up the SFDM formed outside the Dacron® mesh which was in contact with the reactor biomass (external cake). Particle size distributions (PDS) were determined by a Mastersizer 3000 laser diffraction particle size analyser from Malvern Instruments (UK). Freshly collected samples were dispersed in deionized water at the lowest stirring speed adequate for resuspension minimizing the effect of the induced shear stress on the particle size distribution and analysed.

Recovery of the microbiota for microbiological analysis

Aliquots of the ESFDM layer, mixed liquor and effluent were sampled under sterile conditions for microbiological analysis of the ESFDM and e-ESFDM bioreactors. Serial dilutions of the samples were performed for the mixed liquor and ESFDM layer samples. The diluted samples were spread on Petri dishes (14 cm diameter) containing Plate Count Agar (PCA: 5 g peptone, 2.5 g yeast extract, 1 g D-glucose, 15 g agar, 1 L deionized water) or Yeast Extract Peptone Dextrose (YEPD: 20 g D-glucose, 20 g Peptone, 10 g yeast extract, 20 agar, 1 L deionized water) media specific for fungi. Microbial growth was done in aerobiosis at room temperature (25°C). Effluent samples (500 mL) were filtered through sterile nitrocellulose membrane filters with a pore size of 0.45 μm and then inoculated and incubated under the above-described conditions. Endospore-forming bacteria were selected by heating undiluted samples to 80 °C for 15 min. Samples obtained by serial dilutions were then spread on PCA medium and grown aerobically at 25 °C.

Quantification and isolation of microorganisms

The total number of culturable microorganisms was determined according to Standard 9215 C[77]. Microbial density was calculated by relating the colony-forming units (CFU) to grams of dry weight (layer and mixed liquor) or mL (effluent). Purification to homogeneity of isolated colonies was conducted by repeated passages through Petri dishes and by morphological analysis by Gram staining and microscopy.

Taxonomical analysis of microorganisms

DNA extraction from purified colonies and amplification by polymerase chain reaction (PCR) were conducted using REDExtract-N-Amp Plant PCR Kit (Merck Life Science Srl, Milan-Italy). The pairs of universal primers com1/com2were used for amplification, specific for highly variable regions V4-V5 of bacterial 16S rDNA, and ITS1 and ITS4 for amplification of internal transcribed spacers ITS2 and ITS1 of fungal 18S rDNA[78,79] All PCR reactions were performed in a 20 mL reaction mixture containing ~50–100 ng of total genomic, according to the manufacturer's instructions and melting temperature of primers, as follows: 5 min of initial denaturation at 94 °C, followed by 35 cycles at 94 °C for 1 min, 60 °C for 1 min and 72 °C for 1 min. The final extension was set at 72 °C for 7 min. PCR products were separated by electrophoresis on 1% agarose gels and recovered using the Qiaex II DNA purification kit (QIAGEN). Sequencing of amplified regions was carried out as a service of Eurofins genomics (https://eurofinsgenomics.eu/). To determine the diversity of species in the ESFDM layer, effluent, and mixed liquor the sequences were aligned by the nucleotide basic local alignment search tool (BLASTn) program of National Center for Biotechnology Information (NCBI, https://www.ncbi.nlm.nih.gov/). The diversity of a community of microorganisms was also expressed in terms of Shannon Index (H) and reciprocal of Simpson's Index (1/D).

REFERENCES

1. Radjenović, J., Matošić, M., Mijatović, I., Petrović, M. & Barceló, D. In *Emerging Contaminants from Industrial and Municipal Waste: Removal Technologies* (eds. Barceló, D. & Petrovic, M.) 37–101 (Springer Berlin Heidelberg, 2008).
2. Cheng, D. et al. Anaerobic membrane bioreactors for antibiotic wastewater treatment: performance and membrane fouling issues. *Bioresour. Technol.* **267**, 714–724 (2018).
3. Dvořák, L., Gómez, M., Dolina, J. & Černín, A. Anaerobic membrane bioreactors—a mini review with emphasis on industrial wastewater treatment: applications, limitations and perspectives. *Desalination Water Treat.* **57**, 19062–19076 (2016).
4. Long, F. et al. Non-woven operational stability of dynamic membrane bioreactor and its fluence factors. *Adv. Mater. Res.* **608–609**, 320–323 (2013).
5. Liu, B., Gu, Y., Kong, L. & Zhang, Y. Evaluation of nano-structured $Ir_{0.5}Mn_{0.5}O_2$ as a potential cathode for intermediate temperature solid oxide fuel cell. *J. Power Sources* **185**, 946–951 (2008).
6. Jolis, D., Hirano, R. & Pitt, P. Tertiary treatment using microfiltration and UV disinfection for water reclamation. *Water Environ. Res.* **71**, 224–231 (1999).
7. Poostchi, A. A., Mehrnia, M. R. & Rezvani, F. Dynamic membrane behaviours during constant flux filtration in membrane bioreactor coupled with mesh filter. *Environ. Technol.* **36**, 1751–1758 (2015).
8. Li, F., Chen, J. & Deng, C. The kinetics of crossflow dynamic membrane bioreactor. *Water SA* **32**, 199–203 (2006).
9. Sreeda, P., Sathya, A. B. & Sivasubramanian, V. Novel application of high-density polyethylene mesh as self-forming dynamic membrane integrated into a bioreactor for wastewater treatment. *Environ. Technol.* **39**, 51–58 (2018).
10. Sabaghian, M., Mehrnia, M. R., Esmaieli, M. & Noormohammadi, D. Formation and performance of self-forming dynamic membrane (SFDM) in membrane bioreactor (MBR) for treating low-strength wastewater. *Water Sci. Technol.* **78**, 904–912 (2018).
11. Castrogiovanni, F. et al. Innovative encapsulated self-forming dynamic biomembrane bioreactor (ESFDMBR) for efficient wastewater treatment and fouling control. *Sci. Total Environ.* 150296. https://doi.org/10.1016/j.scitotenv.2021.150296 (2021).
12. Kooijman, G. et al. Impact of coagulant and flocculant addition to an anaerobic dynamic membrane bioreactor (AnDMBR) treating waste-activated sludge. *Membranes* **7**, 18–29 (2017).
13. Ersahin, M. E., Ozgun, H., Tao, Y. & van Lier, J. B. Applicability of dynamic membrane technology in anaerobic membrane bioreactors. *Water Res* **48**, 420–429 (2014).
14. Hu, Y. et al. Effects of powdered activated carbon addition on filtration performance and dynamic membrane layer properties in a hybrid DMBR process. *Chem. Eng. J.* https://doi.org/10.1016/j.cej.2017.06.072 (2017).
15. Hu, Y. et al. Characterization of a hybrid powdered activated carbon-dynamic membrane bioreactor (PAC-DMBR) process with high flux by gravity flow: operational performance and sludge properties. *Bioresour. Technol.* **223**, 65–73 (2017).
16. Borea, L., Naddeo, V. & Belgiorno, V. Application of electrochemical processes to membrane bioreactors for improving nutrient removal and fouling control. *Environ. Sci. Pollut. Res.* **24**, 321–333 (2017).
17. Ensano, B. M. B. et al. Removal of pharmaceuticals from wastewater by intermittent electrocoagulation. *Water Switz* **9**, 85–100 (2017).
18. Corpuz, M. V. A. et al. Viruses in wastewater: occurrence, abundance and detection methods. *Sci. Total Environ.* **745**, 140910 (2020).
19. Buonerba, A. et al. Coronavirus in water media: Analysis, fate, disinfection and epidemiological applications. *J. Hazard. Mater.* **415**, 125580 (2021).
20. Zhang, J. et al. Low-voltage electric field applied into MBR for fouling suppression: performance and mechanisms. *Chem. Eng. J.* **273**, 223–230 (2015).
21. Ibeid, S., Elektorowicz, M. & Oleszkiewicz, J. A. Novel electrokinetic approach reduces membrane fouling. *Water Res* **47**, 6358–6366 (2013).
22. Ensano, B. M. B. et al. Combination of electrochemical processes with membrane bioreactors for wastewater treatment and fouling Control: a review. *Front. Environ. Sci* **4**, 1–15 (2016).
23. Borea, L., Naddeo, V., Belgiorno, V. & Choo, K. H. Control of quorum sensing signals and emerging contaminants in electrochemical membrane bioreactors. *Bioresour. Technol.* **269**, 89–95 (2018).

24. Jiang, W., Xia, S., Liang, J., Zhang, Z. & Hermanowicz, S. W. Effect of quorum quenching on the reactor performance, biofouling and biomass characteristics in membrane bioreactors. *Water Res* **47**, 187–196 (2013).

25. Ensano, B. M. B., Borea, L., Naddeo, V., de Luna, M. D. G. & Belgiorno, V. Control of emerging contaminants by the combination of electrochemical processes and membrane bioreactors. *Environ. Sci. Pollut. Res.* 1–10 https://doi.org/10.1007/s11356-017-9097-z (2017).

26. Xiong, J., Fu, D., Singh, R. P. & Ducoste, J. J. Structural characteristics and development of the cake layer in a dynamic membrane bioreactor. *Sep. Purif. Technol.* **167**, 88–96 (2016).

27. Liang, S., Qu, L., Meng, F., Han, X. & Zhang, J. Effect of sludge properties on the filtration characteristics of self-forming dynamic membranes (SFDMs) in aerobic bioreactors: Formation time, filtration resistance, and fouling propensity. *J. Membr. Sci.* **436**, 186–194 (2013).

28. Bayar, S., Karagunduz, A. & Keskinler, B. Influences of electroosmosis and electrophoresis on permeate flux and membrane fouling in submerged membrane bioreactors (SMBRs). *Water Sci. Technol.* **74**, 766–776 (2016).

29. Liu, J., Liu, L., Gao, B. & Yang, F. Cathode membrane fouling reduction and sludge property in membrane bioreactor integrating electrocoagulation and electrostatic repulsion. *Sep. Purif. Technol.* **100**, 44–50 (2012).

30. Yu, H., Xu, G., Qu, F., Li, G. & Liang, H. Effect of solid retention time on membrane fouling in membrane bioreactor: from the perspective of quorum sensing and quorum quenching. *Appl. Microbiol. Biotechnol.* **100**, 7887–7897 (2016).

31. Hong, P. N., Taing, C., Phan, P. T. & Honda, R. Polarity-molecular weight profile of extracellular polymeric substances in a membrane bioreactor: comparison between bulk sludge and cake layers. *J. Water Environ. Technol.* **16**, 40–53 (2018).

32. Lei, Z., Luo, X., Zhang, Z. & Sugiura, N. Effects of variations of extracellular polymeric substances and soluble microbial products on activated sludge properties during anaerobic storage. *Environ. Technol.* **28**, 529–544 (2007).

33. Wei, V., Oleszkiewicz, J. A. & Elektorowicz, M. Nutrient removal in an electrically enhanced membrane bioreactor. *Water Sci. Technol.* **60**, 3159–3163 (2009).

34. Kim, H. G., Jang, H. N., Kim, H. M., Lee, D. S. & Chung, T. H. Effect of an electro phosphorous removal process on phosphorous removal and membrane permeability in a pilot-scale MBR. *Desalination* **250**, 629–633 (2010).

35. Bani-Melhem, K. & Smith, E. Grey water treatment by a continuous process of an electrocoagulation unit and a submerged membrane bioreactor system. *Chem. Eng. J.* **198–199**, 201–210 (2012).

36. Mohammadi, A. et al. Effectiveness of nanozeolite modified by cationic surfactant in the removal of disinfection by-product precursors from water solution. *Int. J. Environ. Health Eng.* **1**, 3–3 (2012).

37. Albrektienė, R., Rimeika, M., Zalieckienė, E., Šaulys, V. & Zagorskis, A. Determination of organic matter by UV absorption in the ground water. *J. Environ. Eng. Landsc. Manag.* **20**, 163–167 (2012).

38. Plakas, K. V., Karabelas, A. J., Wintgens, T. & Melin, T. A study of selected herbicides retention by nanofiltration membranes-the role of organic fouling. *J. Membr. Sci.* **284**, 291–300 (2006).

39. Yuan, W. & Zydney, A. L. Humic acid fouling during microfiltration. *J. Membr. Sci.* **157**, 1–12 (1999).

40. Nikolaou, A. D., Golfinopoulos, S. K., Lekkas, T. D. & Kostopoulou, M. N. DBP levels in chlorinated drinking water: effect of humic substances. *Environ. Monit. Assess.* **93**, 301–319 (2004).

41. Kliaugaite, D., Yasadi, K., Euverink, G. J., Bijmans, M. F. M. & Racys, V. Electrochemical removal and recovery of humic-like substances from wastewater. *Sep. Purif. Technol.* **108**, 37–44 (2013).

42. Kourdali, S., Badis, A., Saiba, A., Boucherit, A. & Boutoumi, H. Humic acid removal by electrocoagulation using aluminium sacrificial anode under influencing operational parameters. *Desalination Water Treat.* **52**, 5442–5453 (2014).

43. Wang, Y. K., Sheng, G. P., Shi, B. J., Li, W. W. & Yu, H. Q. A novel electrochemical membrane bioreactor as a potential net energy producer for sustainable wastewater treatment. *Sci. Rep.* **3**, 21–26 (2013).

44. Zeyoudi, M. et al. Impact of continuous and intermittent supply of electric field on the function and microbial community of wastewater treatment electro-bioreactors. *Electrochim. Acta* **181**, 271–279 (2015).

45. Luo, J. et al. Succession of biofilm communities responsible for biofouling of membrane bio-reactors (MBRs). *PLoS ONE* **12**, e0179855 (2017).

46. Sato, Y. et al. Transition of microbial community structures after development of membrane fouling in membrane bioreactors (MBRs). *AMB Express* **10**, 18 (2020).

47. Zhang, H., Yuan, X., Wang, H., Ma, S. & Ji, B. Performance and microbial community of different biofilm membrane bioreactors treating antibiotic-containing synthetic mariculture wastewater. *Membranes* **10**, 282–294 (2020).

48. Qi, K. et al. Development of an electrochemical ceramic membrane bioreactor for the removal of PPCPs from wastewater. *Water* **12**, 1838–1852 (2020).

49. Lee, S. H., Hong, T. I., Kim, B., Hong, S. & Park, H. D. Comparison of bacterial communities of biofilms formed on different membrane surfaces. *World J. Microbiol. Biotechnol.* **30**, 777–782 (2014).

50. Jo, S. J., Kwon, H., Jeong, S. Y., Lee, C. H. & Kim, T. G. Comparison of microbial communities of activated sludge and membrane biofilm in 10 full-scale membrane bioreactors. *Water Res.* **101**, 214–225 (2016).

51. Lim, S. Y. et al. Correlation between microbial community structure and biofouling in a laboratory scale membrane bioreactor with synthetic wastewater. *Desalination* **287**, 209–215 (2012).

52. Wiencek, K. M., Klapes, N. A. & Foegeding, P. M. Hydrophobicity of Bacillus and Clostridium spores. *Appl. Environ. Microbiol.* **56**, 2600–2605 (1990).

53. Lade, H., Paul, D. & Kweon, J. H. Isolation and molecular characterization of biofouling bacteria and profiling of quorum sensing signal molecules from membrane bioreactor activated sludge. *Int. J. Mol. Sci.* **15**, 2255–2273 (2014).

54. Fitriyah, D., Wahyudi, A. T. & Rusmana, I. Characterization of bacteria producing Acyl Homoserine Lactone (AHL) lactonase from agricultural lands. *Adv. Environ. Biol.* **9**, 140–148 (2015).

55. Xu, F., Zhao, C., Lee, C. H., Wang, W. & Xu, Q. Anti-biofouling performance of an immobilized indigenous quorum quenching bacterium bacillus cereus hg10 and its influence on the microbial community in a bioreactor. *Int. J. Environ. Res. Public. Health* **16**, 8–10 (2019).

56. Ishizaki, S., Sugiyama, R. & Okabe, S. Membrane fouling induced by AHL-mediated soluble microbial product (SMP) formation by fouling-causing bacteria co-cultured with fouling-enhancing bacteria. *Sci. Rep.* **7**, 1–8 (2017).

57. Jiang, B. et al. Impacts of long-term electric field applied on the membrane fouling mitigation and shifts of microbial communities in EMBR for treating phenol wastewater. *Sci. Total Environ.* **716**, 137139 (2020).

58. Feng, Y., Feng, J. & Shu, Q. L. Isolation and characterization of heterotrophic nitrifying and aerobic denitrifying Klebsiella pneumoniae and Klebsiella variicola strains from various environments. *J. Appl. Microbiol.* **124**, 1195–1211 (2018).

59. Padhi, S. K. et al. Characterisation of heterotrophic nitrifying and aerobic denitrifying Klebsiella pneumoniae CF-S9 strain for bioremediation of wastewater. *Int. Biodeterior. Biodegrad.* **78**, 67–73 (2013).

60. Li, X. G., Cao, H., Bin, Wu, J. C. & Yu, K. T. Inhibition of the metabolism of nitrifying bacteria by direct electric current. *Biotechnol. Lett.* **23**, 705–709 (2001).

61. Wan, W., He, D. & Xue, Z. Removal of nitrogen and phosphorus by heterotrophic nitrification-aerobic denitrification of a denitrifying phosphorus-accumulating bacterium *Enterobacter cloacae* HW-15. *Ecol. Eng.* **99**, 199–208 (2017).

62. Padhi, S. K., Tripathy, S., Mohanty, S. & Maiti, N. K. Aerobic and heterotrophic nitrogen removal by *Enterobacter cloacae* CF-S27 with efficient utilization of hydroxylamine. *Bioresour. Technol.* **232**, 285–296 (2017).

63. Yang, Y., Qiao, S., Jin, R., Zhou, J. & Quan, X. A novel aerobic electrochemical membrane bioreactor with CNTs hollow fiber membrane by electrochemical oxidation to improve water quality and mitigate membrane fouling. *Water Res.* **151**, 54–63 (2019).

64. Mendes Predolin, L., Moya-Llamas, M. J., Vásquez-Rodríguez, E. D., Trapote Jaume, A. & Prats Rico, D. Effect of current density on the efficiency of a membrane electro-bioreactor for removal of micropollutants and phosphorus, and reduction of fouling: a pilot plant case study. *J. Environ. Chem. Eng.* **9**, 104874 (2021).

65. Bayramoglu, M., Kobya, M., Can, O. T. & Sozbir, M. Operating cost analysis of electrocoagulation of textile dye wastewater. *Sep. Purif. Technol.* **37**, 117–125 (2004).

66. Corpuz, M. V. A. et al. Wastewater treatment and fouling control in an electro algae-activated sludge membrane bioreactor. *Sci. Total Environ.* **786**, 147475 (2021).

67. Li, J., Zhang, X., Cheng, F. & Liu, Y. New insights into membrane fouling in submerged MBR under sub-critical flux condition. *Bioresour. Technol.* **137**, 404–408 (2013).

68. Li, X., Gao, F., Hua, Z., Du, G. & Chen, J. Treatment of synthetic wastewater by a novel MBR with granular sludge developed for controlling membrane fouling. *Sep. Purif. Technol.* **46**, 19–25 (2005).

69. Yang, P. Y., Cao, K. & Kim, S. J. Entrapped mixed microbial cell process for combined secondary and tertiary wastewater treatment. *Water Environ. Res.* **74**, 226–234 (2002).

70. Borea, L. et al. Are pharmaceuticals removal and membrane fouling in electro-membrane bioreactor affected by current density? *Sci. Total Environ.* **692**, 732–740 (2019).

71. APAT and CNR-IRSA. Metodi analitici per le acque. Manuali e Linee Guida 29/2003. (2003).

72. de la Torre, T., Lesjean, B., Drews, A. & Kraume, M. Monitoring of transparent exopolymer particles (TEP) in a membrane bioreactor (MBR) and correlation with other fouling indicators. *Water Sci. Technol.* **58**, 1903–1909 (2008).

73. Le-Clech, P., Chen, V. & Fane, T. A. G. Fouling in membrane bioreactors used in wastewater treatment. *J. Membr. Sci.* **284**, 17–53 (2006).

74. Morgan, J. W., Forster, C. F. & Evison, L. A comparative study of the nature of biopolymers extracted from anaerobic and activated sludges. *Water Res.* **24**, 743–750 (1990).

75. Frølund, B., Griebe, T. & Nielsen, P. H. Enzymatic activity in the activated-sludge floc matrix. *Appl. Microbiol. Biotechnol.* **43**, 755–761 (1995).

76. DuBois, M., Gilles, K. A., Hamilton, J. K., Rebers, P. A. & Smith, F. Colorimetric method for determination of sugars and related substances. *Anal. Chem.* **28**, 350–356 (1956).

77. 9215 HETEROTROPHIC PLATE COUNT (2017). in *Standard Methods For the Examination of Water and Wastewater* (American Public Health Association, 2018). https://doi.org/10.2105/SMWW.2882.188.

78. Vigliotta, G. et al. Natural merodiploidy involving duplicated rpoB alleles affects secondary metabolism in a producer actinomycete. *Mol. Microbiol.* **55**, 396–412 (2005).

79. White, T. J., Bruns, T., Lee, S. & Taylor, J. In *PCR Protocols* (eds. Innis, M. A., Gelfand, D. H., Sninsky, J. J. & White, T. J.) 315–322 (Academic Press, 1990).

ACKNOWLEDGEMENTS

AUTHOR CONTRIBUTIONS

J.M.J.M.-M., M.V.A.C., L.B., C.C., G.V., T.Z., and A.B. conducted experiments and data analysis. M.V.A.C., L.B., M.D.G.D.L., F.B., S.W.H., G.V.K., G.V., T.Z., A.B., V.B. and V.N. contributed to manuscript preparation, review and editing. V.B. and V.N. provided funding. All the authors have read and approved the manuscript.

COMPETING INTERESTS

The authors declare no competing interests.

ADDITIONAL INFORMATION

Supplementary information The online version contains supplementary material available at https://doi.org/10.1038/s41545-022-00184-z.

Correspondence and requests for materials should be addressed to Antonio Buonerba or Vincenzo Naddeo.

Reprints and permission information is available at http://www.nature.com/reprints

Publisher's note Springer Nature remains neutral with regard to jurisdictional claims in published maps and institutional affiliations.